



**Comparison of Electromagnetic Simulation Results
with Experimental Data for an Aperture-Coupled
C-band Patch Antenna**

**by Steven Keller, William Coburn,
Theodore Anthony, and Chad Patterson**

ARL-TR-3994

November 2006

NOTICES

Disclaimers

The findings in this report are not to be construed as an official Department of the Army position unless so designated by other authorized documents.

Citation of manufacturer's or trade names does not constitute an official endorsement or approval of the use thereof.

Destroy this report when it is no longer needed. Do not return it to the originator.

Army Research Laboratory

Adelphi, MD 20783-1197

ARL-TR-3994

November 2006

**Comparison of Electromagnetic Simulation Results
with Experimental Data for an Aperture-Coupled
C-band Patch Antenna**

**Steven Keller, William Coburn, Theodore Anthony,
and Chad Patterson
Sensors and Electron Devices Directorate, ARL**

Approved for public release; distribution unlimited.

REPORT DOCUMENTATION PAGE

*Form Approved
OMB No. 0704-0188*

Public reporting burden for this collection of information is estimated to average 1 hour per response, including the time for reviewing instructions, searching existing data sources, gathering and maintaining the data needed, and completing and reviewing the collection information. Send comments regarding this burden estimate or any other aspect of this collection of information, including suggestions for reducing the burden, to Department of Defense, Washington Headquarters Services, Directorate for Information Operations and Reports (0704-0188), 1215 Jefferson Davis Highway, Suite 1204, Arlington, VA 22202-4302. Respondents should be aware that notwithstanding any other provision of law, no person shall be subject to any penalty for failing to comply with a collection of information if it does not display a currently valid OMB control number.

PLEASE DO NOT RETURN YOUR FORM TO THE ABOVE ADDRESS.

1. REPORT DATE (DD-MM-YYYY) November 2006		2. REPORT TYPE Final		3. DATES COVERED (From - To) June to September 2006	
4. TITLE AND SUBTITLE Comparison of Electromagnetic Simulation Results with Experimental Data for an Aperture-Coupled C-band Patch Antenna				5a. CONTRACT NUMBER	
				5b. GRANT NUMBER	
				5c. PROGRAM ELEMENT NUMBER	
6. AUTHOR(S) Steven Keller, William Coburn, Theodore Anthony, and Chad Patterson				5d. PROJECT NUMBER	
				5e. TASK NUMBER	
				5f. WORK UNIT NUMBER	
7. PERFORMING ORGANIZATION NAME(S) AND ADDRESS(ES) U.S. Army Research Laboratory ATTN: AMSRD-ARL-SE-RM 2800 Powder Mill Road Adelphi, MD 20783-1197				8. PERFORMING ORGANIZATION REPORT NUMBER ARL-TR-3994	
9. SPONSORING/MONITORING AGENCY NAME(S) AND ADDRESS(ES) U.S. Army Research Laboratory 2800 Powder Mill Road Adelphi, MD 20783-1197				10. SPONSOR/MONITOR'S ACRONYM(S)	
				11. SPONSOR/MONITOR'S REPORT NUMBER(S)	
12. DISTRIBUTION/AVAILABILITY STATEMENT Approved for public release; distribution unlimited.					
13. SUPPLEMENTARY NOTES					
14. ABSTRACT The Method of Moments, implemented in 2.5-dimensions (2.5-D) with the multilayer Green's Function, and the Finite Element Method, a fully three-dimensional (3-D) solution of Maxwell's equations, are two popular methods for antenna simulations. Commercial software implementing these two methods was used to simulate a single aperture-coupled patch antenna element. This effort was time limited so that a simple antenna was selected for which the antenna design, fabrication, and measurements could be accomplished in less than three months. The simulation results are compared with experimental data measured for an antenna prototype that has substrate and ground plane dimensions of 4 inches by 4 inches. The microstrip feed line extends to the edge of the substrate where a coaxial connector is installed between the microstrip and slotted ground plane and there is no bottom ground plane. The results are used to compare and contrast the use of these two approaches for the design and simulation of an aperture-coupled patch antenna with finite size substrate and ground plane.					
15. SUBJECT TERMS Aperture coupled patch, impedance bandwidth, microstrip, FEKO, EMPiCASSO					
16. SECURITY CLASSIFICATION OF:			17. LIMITATION OF ABSTRACT UL	18. NUMBER OF PAGES 24	19a. NAME OF RESPONSIBLE PERSON Steven Keller
a. REPORT Unclassified	b. ABSTRACT Unclassified	c. THIS PAGE Unclassified			19b. TELEPHONE NUMBER (Include area code) (301) 394-2705

Contents

List of Figures	iv
List of Tables	iv
Acknowledgment	v
1. Introduction	1
2. EMPiCASSO Simulation	1
3. HFSS Simulation	3
4. Experimental Data	5
4.1 Network Analyzer Measurements	5
4.2 Antenna Pattern Measurements	5
5. Results	8
6. Conclusion	13
7. References	14
Distribution List	15

List of Figures

Figure 1. An aperture-coupled patch antenna design in EMPiCASSO showing (a) the substrate configuration and (b) the mesh discretization.	2
Figure 2. Aperture-coupled patch antenna model in HFSS showing the 3-D model and the radiation boundary.	3
Figure 3. Radiation pattern measurement setup in the anechoic chamber.....	6
Figure 4. Schematic diagram of antenna measurements with the substitution method.	7
Figure 5. VSWR comparison for an aperture-coupled C-band patch antenna.	8
Figure 6. S_{11} comparison for an aperture-coupled C-band patch antenna.	9
Figure 7. Measured realized gain compared to EMP directivity and HFSS realized gain for an aperture-coupled C-band patch antenna.....	10
Figure 8. Measured gain compared to EMP and HFSS directivity for an aperture coupled C-band patch antenna.....	11
Figure 9. E-Plane radiation pattern comparison at 4.55 GHz.	12
Figure 10. H-Plane radiation pattern comparison at 4.55 GHz.....	12

List of Tables

Table 1. Aperture-coupled patch antenna design parameters.	2
Table 2. HFSS simulation parameters for an aperture-coupled patch antenna.....	4
Table 3. Typical parameters obtained for antenna measurements.....	7

Acknowledgment

The authors would like to thank Russell Harris of the Army Research Laboratory (ARL) for converting the antenna geometry into fabrication drawings and for constructing the prototype. Steven Weiss of ARL provided guidance and advice in the antenna measurements along with a critical review of the manuscript. Their assistance on this project was greatly appreciated.

INTENTIONALLY LEFT BLANK.

1. Introduction

With the large number of electromagnetic (EM) simulation software packages available for use in antenna design, which use different numerical techniques in the time or frequency domain, it is often difficult to determine which program will work best for a given antenna geometry. For multilayer planar structures, the Method of Moments (MoM) or Finite Element Method are quite popular. In order to streamline the antenna design process and generate accurate results before prototype construction, it is important to select an EM simulation program that will provide an optimal balance between a minimal simulation run time and a maximized correlation between the simulation results and the experimental data. An aperture-coupled *C*-band patch antenna is designed and simulated with both *EMAG Technologies* EMPiCASSO (EMP) (1) and *Ansoft's* High Frequency Structure Simulator (HFSS) (2). These codes were chosen as representative of the MoM implemented in 2.5-dimensions (2.5-D) with the multilayer Green's Function (EMP) and the FEM, a fully three-dimensional (3-D) solution of Maxwell's equations (HFSS). These simulation results are compared with experimental data measured for an antenna prototype that has substrate and ground plane dimensions 4 inches by 4 inches. The feed line extends to the edge of the substrate where a coaxial connector is installed between the feed and slotted ground plane and there is no bottom ground plane. The results are used to compare and contrast the use of EMP and HFSS for the design and simulation of an aperture-coupled patch antenna with finite size substrate and ground plane. This effort was time limited so that a simple patch design was chosen for which the antenna design, fabrication, and measurements could be accomplished in less than three months.

2. EMPiCASSO Simulation

A *C*-band patch antenna was designed as a 2.5-D model in EMP to operate with a resonant frequency between 4.4 and 5 GHz. Since the patch antenna is inherently a narrowband structure, it was not expected to cover this entire band, so the design focused on the center frequency around 4.6 GHz corresponding to a free-space wavelength, $\lambda_0 = 2.57$ inches. The goal in the antenna design was to position the center frequency around 4.6 GHz and maximize the -10 -dB return loss bandwidth. The final antenna design is shown in figure 1 with the detailed dimensions and substrate layer properties listed in table 1. The relative dielectric constant of the substrate layers were set to $\epsilon_r = 2.33$ to represent Rogers RT/duroid¹ 5870 low-loss dielectric (3). Then the effective wavelength in the substrate, $\lambda_{eff} = \lambda_0/\sqrt{\epsilon_r} = 1.68$ inches is used for mesh refinement in the aperture and on the microstrip feed with 80 samples/ λ_{eff} rather than the default

¹ Duroid is a registered trademark of Rogers Corporation.

30 samples. The 5870 substrate is 2-oz copper clad amounting to about 70 μm copper thickness, and the different layers are bonded with 3M Scotch² adhesive transfer tape³.

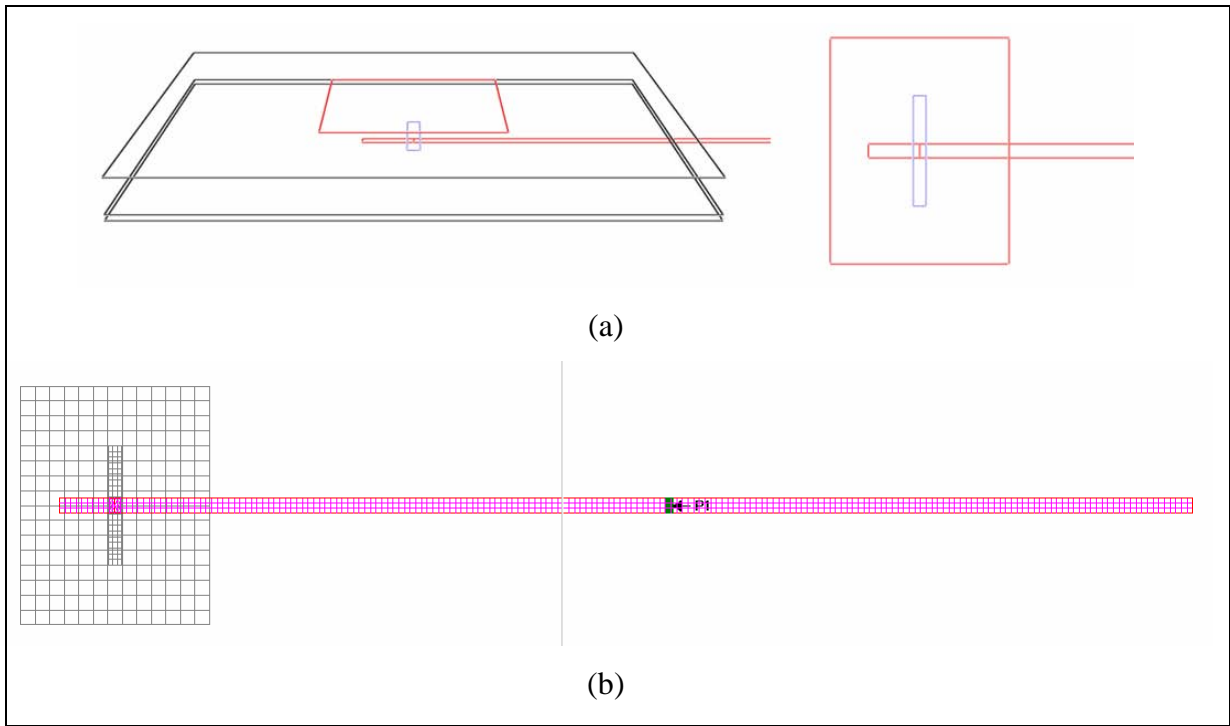


Figure 1. An aperture-coupled patch antenna design in EMPiCASSO showing (a) the substrate configuration and (b) the mesh discretization.

Table 1. Aperture-coupled patch antenna design parameters.

Layer Description	Dimensions and Substrate Thickness (mil)
Patch (Copper)	680- by 860-mil patch
Upper Substrate (RT/duroid)	4000 by 4000 mils, 125-mil thickness
Slotted Ground Plane (Copper)	4000 by 4000 mils with 50- by 430-mil slot
Lower Substrate (RT/duroid)	4000 by 4000 mils, 20-mil thickness
Microstrip Feed Line (Copper)	55-mil width, 2200-mil total length extending 200 mils past slot center

² 3M and Scotch are registered trademarks of 3M Corporation.

³ http://solutions.3m.com/en_US/.

The design involved a number of modeling approximations, including an infinite slotted ground plane and infinite substrate, with a feed line trace that EMP automatically extends to $\sim 2\lambda_{eff}$ at each excitation frequency. A port excitation was placed along this feedline roughly at the center and simulated with the MoM technique in EMP. A convergence study showed that the default mesh size was sufficient except for the slot and microstrip feed line where mesh refinement is needed to improve accuracy. The simulation took ~ 30 seconds per frequency or about 10 minutes to complete a 21-point sweep from 4.4 to 4.8 GHz. The 2.5-D simulation results are compared to the experimental data for a prototype antenna fabricated on a 4-inch-square substrate.

3. HFSS Simulation

The aperture-coupled patch antenna that was designed and fine tuned in EMP was then constructed as a 3-D model in HFSS. This model, along with the radiation boundary, is shown in figure 2. The substrate dimensions were set to the as-fabricated antenna dimensions, 4000 by 4000 mils where the feed line extends 2000 mils from the aperture center to the ground plane edge. A coaxial excitation was applied at the end of the feed line rather than a lumped port excitation as in EMP. A radiation boundary was constructed around the model which extended 1500 mils from each edge of the substrate corresponding to $\sim 0.58\lambda_0$.

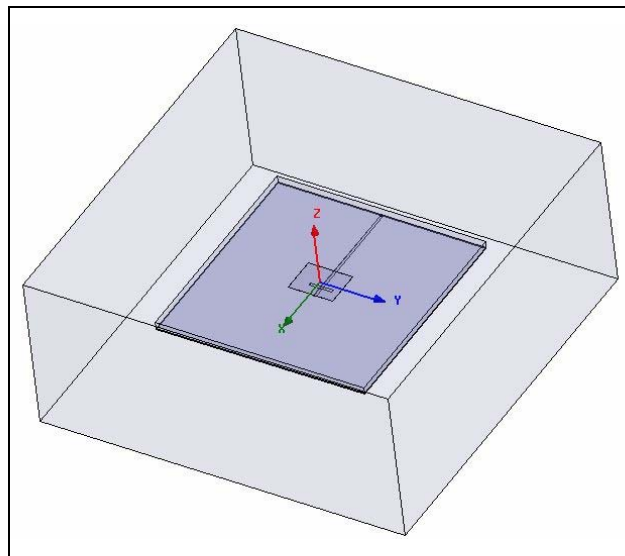


Figure 2. Aperture-coupled patch antenna model in HFSS showing the 3-D model and the radiation boundary.

A number of different simulations were run with this model, with certain simulation parameters such as the max delta S and the lambda refinement target being altered before each trial run. The max delta S parameter is the criterion for convergence, with the simulation continuing to refine its adaptive mesh until the S-parameters of the simulated solution between two consecutive iterations differ by less than the value of this parameter. Thus, with a smaller max delta S, a stronger convergence criterion will be satisfied, but it will take more adaptive passes to converge and the simulation time will consequently increase. The lambda refinement target parameter sets the approximate size, in wavelengths, of each cell on the adaptive mesh that is created over the simulated structure. Thus, with a smaller lambda refinement target, the adaptive mesh will contain more elements, potentially offering a more accurate solution at the cost of increased simulation run time and increased system memory usage. The details of these simulations are shown in table 2 for a 21-point frequency sweep (4.4 to 4.8 GHz) with 20% maximum mesh refinement per pass.

For each of these parameter choices, a fast and discrete sweep was run to compare simulation sweep methods. The fast-sweep simulation has a much shorter simulation run time than the discrete-sweep simulation, which solves each frequency point separately but consumes far more system memory. For a small frequency range such as used in these simulations, the fast-sweep simulation is ideal from an efficiency standpoint and similar to the EMP run time. The simulation 4 results are used for comparison with the EMP results and with experimental data measured for an antenna prototype.

Table 2. HFSS simulation parameters for an aperture-coupled patch antenna.

Simulation Parameters			Simulation Data			
Simulation	Max Delta S	Lambda Refinement Target	Tetrahedra in Mesh	Passes before Convergence	Run time (min.)	$ S_{11} $ Minimum (dB)
1 – Fast	0.02	0.3333	11841	10	5.5	-32.7
1 – Discrete	0.02	0.3333	14236	11	30	-33.3
2 – Fast	0.01	0.3333	14158	11	6	-36.7
2 – Discrete	0.01	0.3333	17085	12	21	-33.1
3 – Fast	0.02	0.25	18753	9	8	-37.2
3 – Discrete	0.02	0.25	15646	8	19.5	-44.4
4 – Fast	0.01	0.25	18795	9	8.5	-45.4
4 – Discrete	0.01	0.25	27075	11	39	-28.9

4. Experimental Data

A prototype of this aperture-coupled patch antenna design was constructed with an on-site router on RT/duroid substrates, which are then adhesive bonded. The 5870 has a relative dielectric constant of approximately $\epsilon_r = 2.33$ as measured with the split cavity method by Damaskos, Inc.⁴ The return loss data were measured with a network analyzer, and the gain and radiation patterns were measured in an on-site tapered anechoic chamber.

4.1 Network Analyzer Measurements

The dielectric and conductor losses are calculated in HFSS as independent loss mechanisms, but for typical materials, these losses are negligible. The impedance mismatch to the antenna determines the input reflection coefficient, Γ , or in terms of S -parameters, $\Gamma = S_{11}$. Performance is often characterized by the return loss, $RL = 20\log(|\Gamma|)$, or alternatively by the input voltage standing wave ratio, $VSWR = (1 + |\Gamma|)/(1 - |\Gamma|)$. Typical C -Band specifications are $VSWR < 1.6$ over the range 4.4 to 5 GHz corresponding to $RL < -13$ dB. The measured data were obtained with a Wiltron⁵ 37269A vector network analyzer (VNA) calibrated with the Wiltron K-Cal Kit Model 3652. When care is taken to make consistent connections, the measurement repeatability is on the order of ± 0.05 dB which is more than sufficient for research purposes.

4.2 Antenna Pattern Measurements

The radiation pattern and gain measurements were conducted with a C -band standard gain horn (SGH) antenna as the system transmitter and the prototype patch antenna set up on a non-metallic rotating positioner to serve as the receiver. A picture of this procedure is shown in figure 3.

⁴ Damaskos, Inc., Concordville, PA <http://www.damaskosinc.com/>.

⁵ Wiltron Company, Morgan Hill, CA.

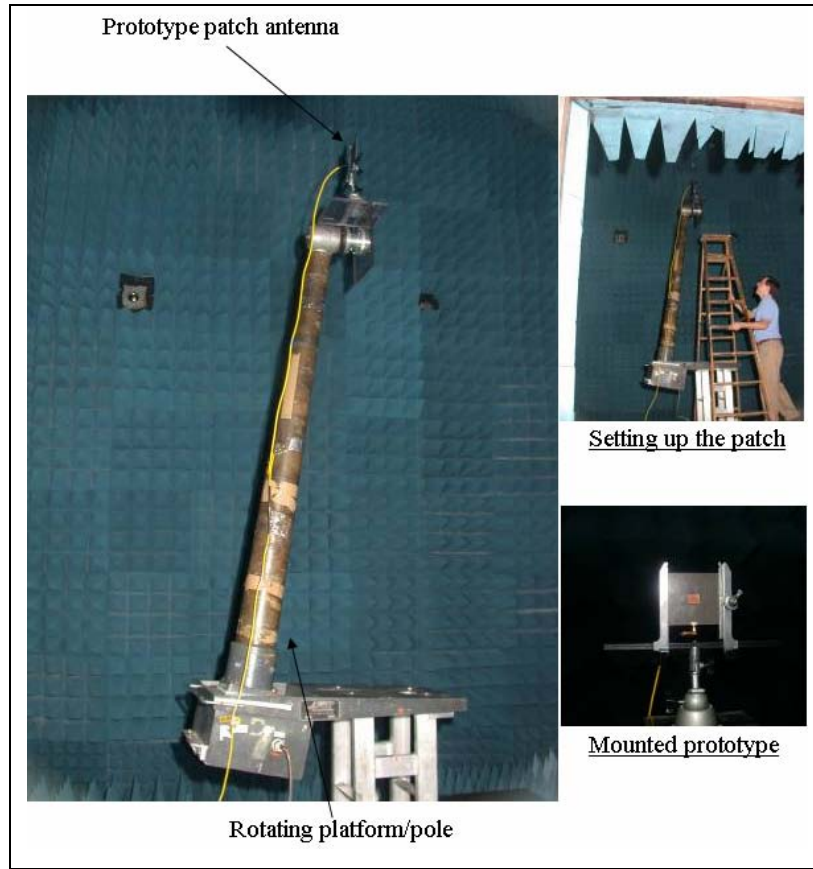


Figure 3. Radiation pattern measurement setup in the anechoic chamber.

We conducted the antenna measurements in an absorber-lined tapered anechoic chamber (4). The length of this chamber is about 50 ft, with the actual distance between transmission and reception antennas being 45.3 ft. Typical component values are shown in table 3 where the equipment is the same between the reference and test setup. Notice that the measured path loss minus the cable and connector attenuation is somewhat less than would be predicted in free space (-64.8 dB). This is a well-known artifact of the guided mode structure in tapered anechoic chambers that is neglected for the purpose of demonstrating antenna performance. A diagram for the antenna pattern measurements is shown in figure 4 with the substitution technique with Narda⁶ SGH antennas. The receiver is phase locked to the transmitter with computer-controlled data acquisition and rotation. The pattern measurements are calibrated according to power meter data versus frequency at the test antenna boresight position. Magnitude and phase data are collected every 1.02 degrees with an accuracy of 0.1 degree, although this does not account for position error in placement of the antenna on the rotator (4).

⁶ <http://www.nardamicrowave.com/east/products.cfm>.

Table 3. Typical parameters obtained for antenna measurements.

	Received with SGH (R_1)	Received with Test Antenna (R_2)
Source (SRC) Output	Typically +6 dBm	Typically +6 dBm
Cable 1 Attenuation	-1 dB	-1 dB
Transmit Antenna (Tx) Gain	15.9 dBi	15.9 dBi
Path Loss	-66.7 dB	-66.7 dB
Receive Antenna (Rx) Gain	15.9 dBi	X
Cable 2 Attenuation	-3 dB	-3 dB
Receiver Attenuation	0 dB	0 dB
Received Power	$R_1 \sim -29$ dBm	R_2 (dBm)
Correction Factor, Δ (dB)	$\Delta = R_2 - R_1 \pm \Delta_{SRC}$	
Test Antenna Gain (dBi)	$G = 15.9 + \Delta$	

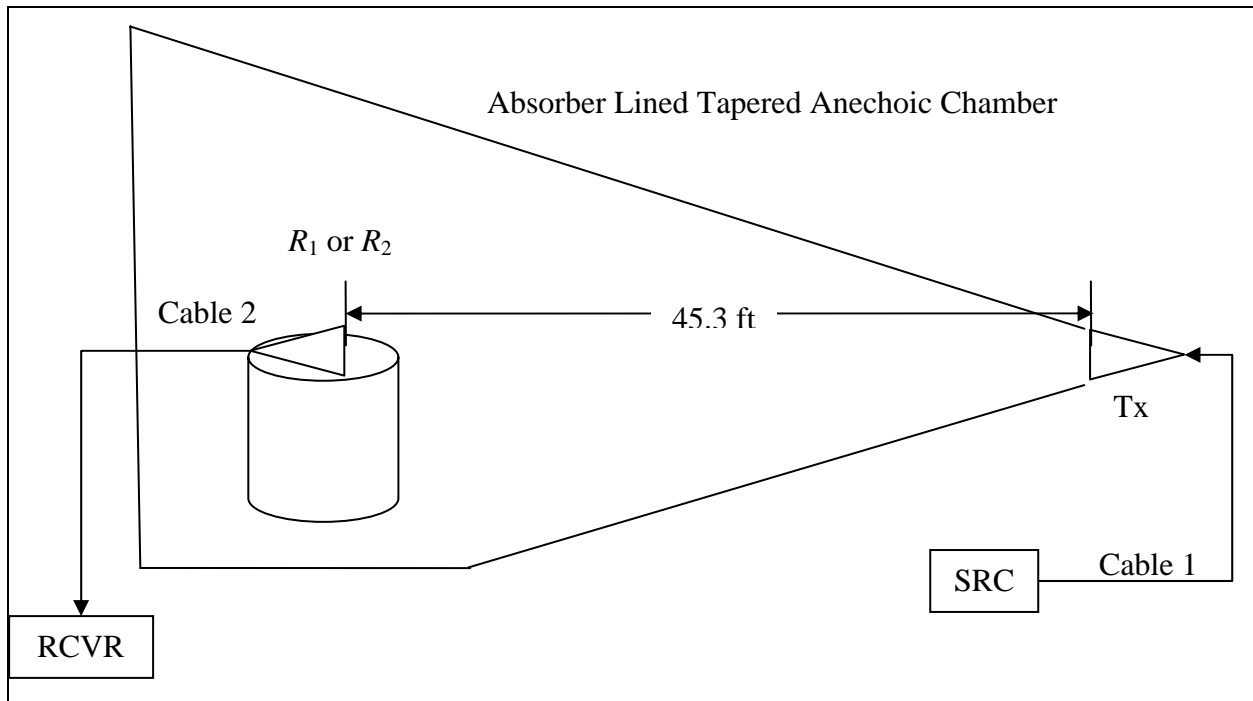


Figure 4. Schematic diagram of antenna measurements with the substitution method.

Two identical Narda SGH antennas that have known gain relative to an isotropic radiator (dBi) over the rated bandwidth are used as the reference antennas. The reception SGH is then replaced with the antenna undergoing test. The exact position of the reference and test antennas on the pylon is a source of uncertainty that is minimized but not completely eliminated. The reception pattern for the radiating antenna is measured versus angle with the experimental error estimated from the repeatability of the data after the antenna is repositioned. The repeatability error can be minimized with careful procedures and placement of the antenna on the rotating pylon but it is not negligible, typically ± 0.25 dB.

5. Results

After the prototype return loss and radiation pattern were measured, the data was then processed and compared with the results from the EMP and HFSS simulations. The VSWR comparison is shown in figure 5 and the corresponding S_{11} comparison is shown in figure 6 for measurements in the range of 4.4 to 4.8 GHz. The EMP simulation results are very close to measurements and this software has been used successfully many times for optimizing an antenna design so that the resulting performance meets the antenna specifications. The HFSS result is shifted -90 MHz to a resonant frequency, $f_r = 4.49$ GHz, so this simulation would suggest a 20-mil smaller patch length ($\sim 3\%$ reduction) to obtain the measured resonance at $f_r = 4.58$ GHz.

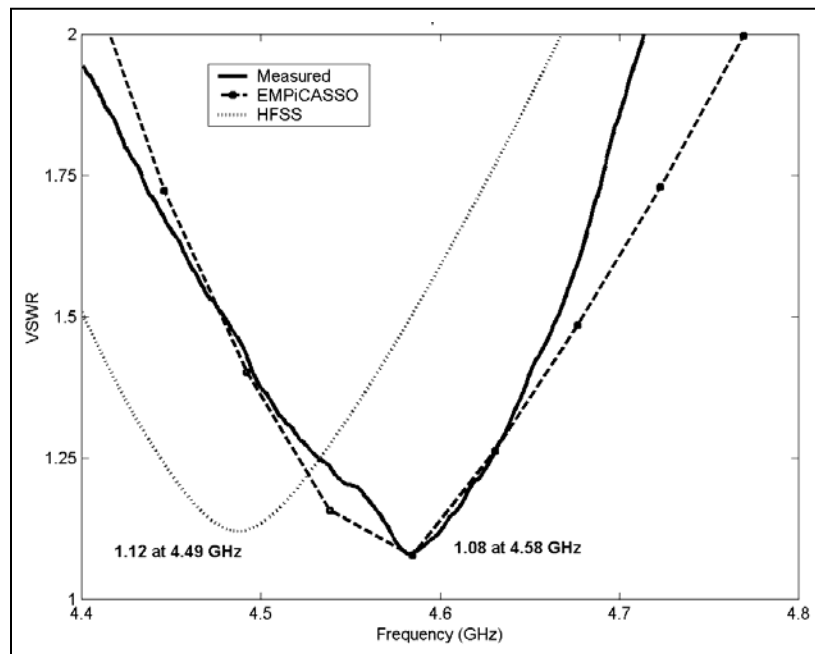


Figure 5. VSWR comparison for an aperture-coupled C-band patch antenna.

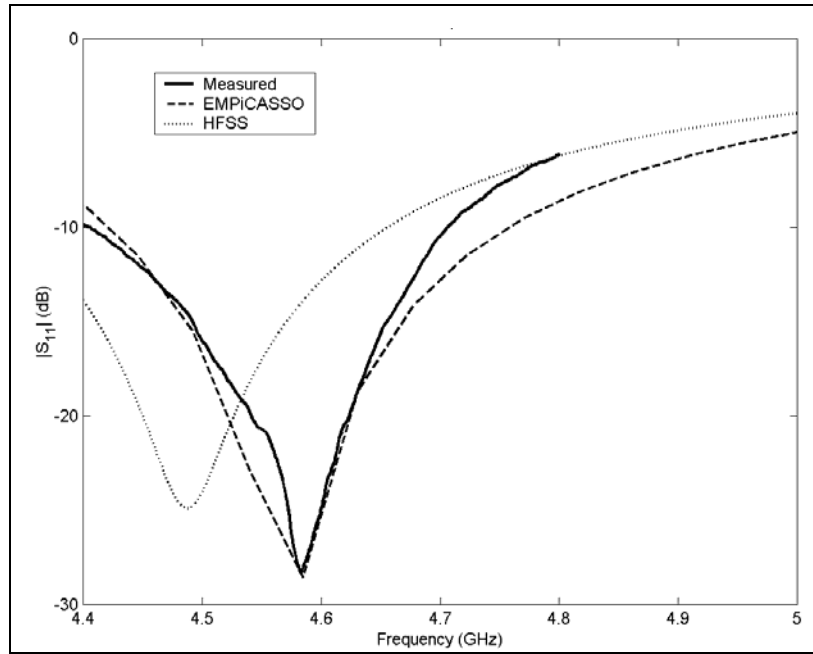


Figure 6. S_{11} comparison for an aperture-coupled C-band patch antenna.

From these plots, it can be seen that the EMP simulation data agree the best with the experimental results. While the -10 -dB return loss bandwidth of the EMP simulation is somewhat larger (330 MHz) than the actual measured bandwidth (300 MHz) of the antenna prototype, the VSWR data are in reasonable agreement between 4.4 GHz and 4.8 GHz, and the simulated center frequency of ~ 4.580 GHz is very close to the measured value of ~ 4.583 GHz.

The HFSS simulation data seem to be moderately consistent in their results, regardless of the simulation parameter values discussed in section 3. The major difference between simulation trials is the return loss value at the resonant frequency. While the discrete sweep simulation 4 resulted in a resonant return loss close to that of the experimentally measured value of -27 dB, the rest of the simulations produced more idealized results between -32 and -45 dB. An important detracting note is that all the HFSS simulation results appear shifted in frequency from the EMP and the experimental results by -90 MHz, with all the simulations displaying resonance at ~ 4.49 GHz. If the HFSS simulation result were shifted 90 MHz, it would be in reasonable agreement with the measured data. The explicit reason for this frequency-shifted aberration is unknown, since the HFSS model dimensions and simulation parameters were exactly the same as the as-fabricated antenna. The difference between EMP and HFSS should only be attributable to the 2.5-D versus a 3-D model of the substrates, and this difference is known to be small and normally neglected.

The measured radiation pattern data are compared to simulated radiation patterns from EMP and HFSS. The measured data correspond to realized gain, G_r , but only directivity is available from

the EMP 2.5-D simulation. Since the antenna losses are small, the EMP directivity should be nearly the same as the gain while the realized gain includes impedance mismatch losses. The directivity is assumed to be equivalent to gain, G_0 ; then it can be converted to G_r based on the calculated reflection coefficient versus frequency, $G_r = G_0 \cdot (1 - |\Gamma|^2)$. HFSS provides directivity, gain, and realized gain, but in these simulations, the observables did not have consistent behavior at all frequencies, which implies that our model is not sufficiently refined to provide accurate radiation calculations. The measured G_r is compared to the EMP and the HFSS directivity and realized gain in figure 7 where the HFSS result is significantly lower than expected.

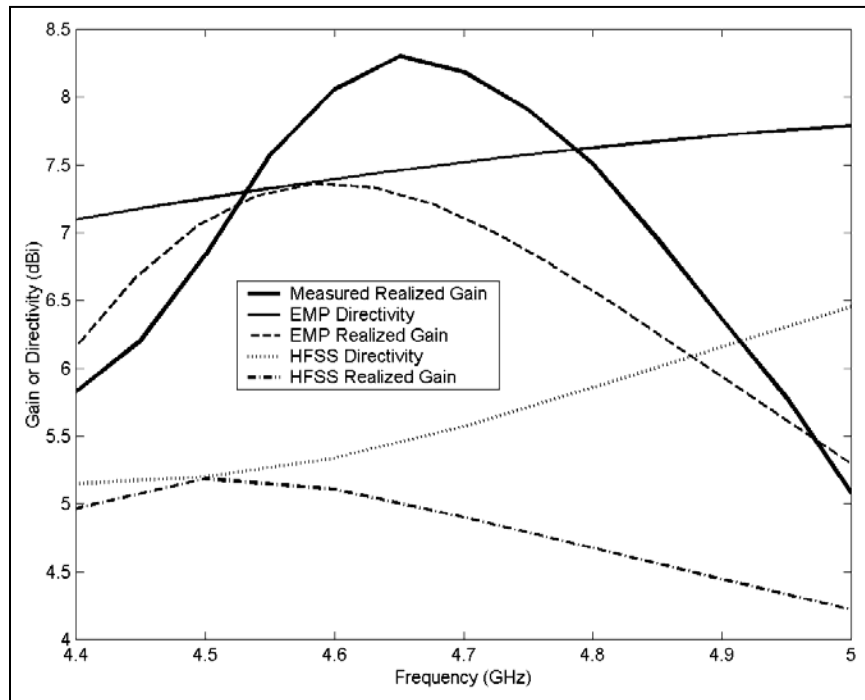


Figure 7. Measured realized gain compared to EMP directivity and HFSS realized gain for an aperture-coupled C-band patch antenna.

The measured G_r is converted to measured gain, G_0 , according to the measured S_{11} data versus frequency, $G_0 = G_r / (1 - |\Gamma|^2)$. A comparison of the measured gain, the EMP and the HFSS gain for a frequency range of 4.4 to 4.8 GHz is shown in figure 8. The G_0 obtained from the measured G_r near the resonant frequency is about 8 dBi, with EMP being in fair agreement at 7.4 dBi, but the HFSS result is significantly lower than measured: only 5.3 dBi. The EMP directivity was in reasonable agreement with measurements whereas the HFSS gain was ~1.5 to 3 dB less than measured. A more detailed investigation of this discrepancy is ongoing where parameter studies of the radiation boundary and layer details are used to further explore the model parameters that most influence the directivity calculated by HFSS.

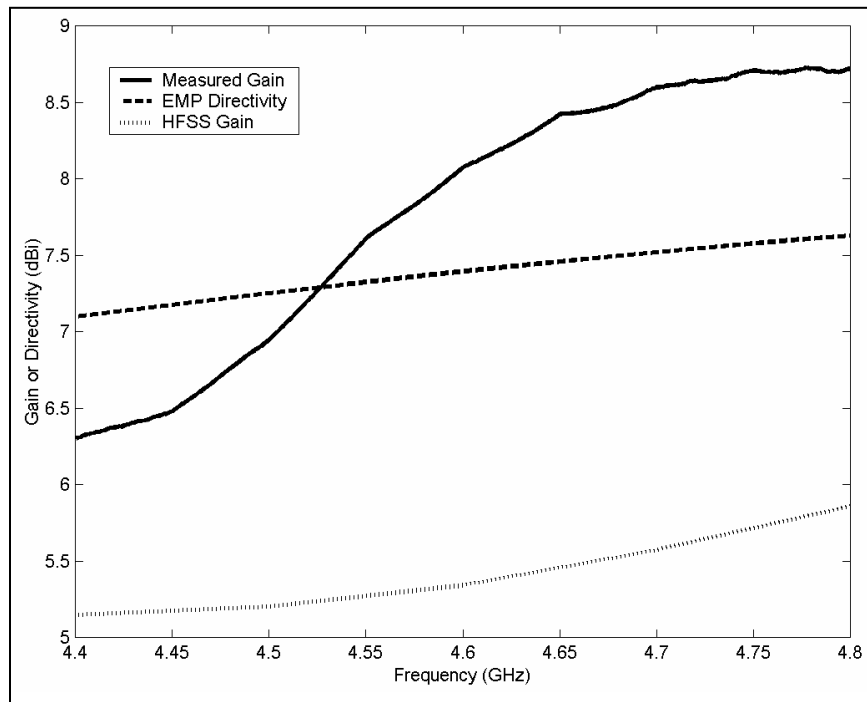


Figure 8. Measured gain compared to EMP and HFSS directivity for an aperture coupled C-band patch antenna.

The measured and simulated radiation patterns at 4.55 GHz are compared in figure 9 for the E-plane pattern and in figure 10 for the H-plane pattern as a function of elevation angle at fixed azimuth. The HFSS simulation results seemed to match the pattern shape of the measured data better than the EMP simulation but seemed to be less accurate for the antenna directivity. EMP had a more idealized pattern and did not predict the reduced gain on boresight observed in the E-plane pattern in the measured and HFSS results. The EMP simulation results tended to match the main lobe reasonably well but did not accurately predict the variations in the back plane radiation. The EMP 2.5-D model has backplane radiation because of leakage through the slotted ground plane rather than the effects of a finite size ground, so these simulation results are as expected. For the E-plane pattern, HFSS has back lobes associated with diffraction effects from the finite ground, but it does not accurately account for backward radiation through the slot. HFSS obtains similar back lobes in the E-plane pattern as measured but for the H-plane has a more idealized back plane pattern. Both methods underestimate the peak back plane radiation level by several decibels.

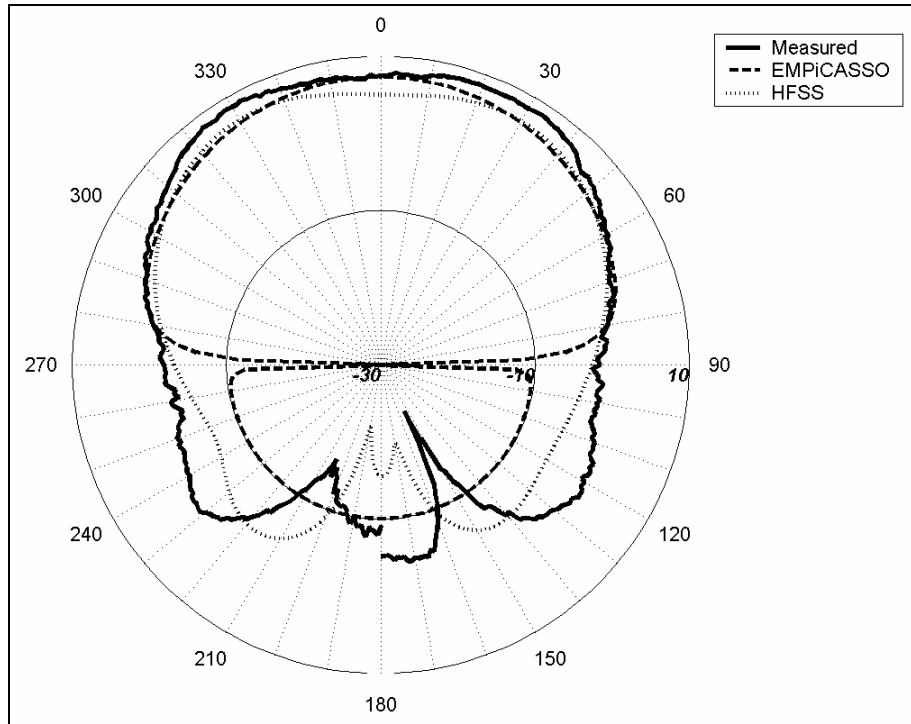


Figure 9. E-Plane radiation pattern comparison at 4.55 GHz.

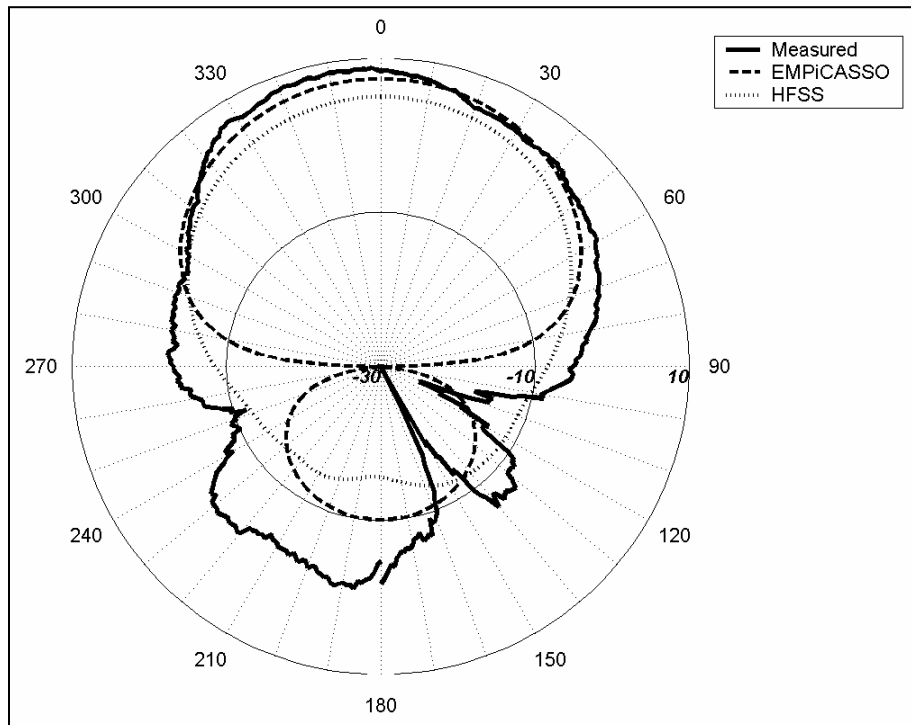


Figure 10. H-Plane radiation pattern comparison at 4.55 GHz.

6. Conclusion

The accuracy and efficiency of the *EMAG* EMPiCASSO and *Ansoft* HFSS software packages were compared with experimental results for an aperture-coupled *C*-band patch antenna geometry. Although the EMP software employed more approximations in its 2.5-D modeling format, it produced far more accurate S-parameter simulation results when compared to measured data than did the HFSS 3-D simulation. The EMP simulation time for a 21-point frequency sweep is on the same order or faster than any of the HFSS simulations performed in this study. While HFSS is widely used to model a variety of antenna structures and provides a moderately accurate solution for this aperture-coupled patch antenna, EMP seems to provide more accurate and more efficient S-parameter solutions. For radiation patterns, the results suggest that neither code will result in an accurate prediction of the true radiation pattern. EMP has reasonable accuracy for simulating front plane radiation, while HFSS may be more useful for simulating back plane radiation. However, in this study neither approach was sufficient for accurately predicting the back plane radiation amplitude or pattern.

The software explored in this paper offers advantages and disadvantages, depending on the parameters that must be simulated. For the antenna input impedance, EMP will offer the most accurate and efficient solution. For gain data, neither program will offer fully accurate results, but EMP appears to be more accurate compared to the measured data. It was expected that the HFSS 3-D model would provide more accurate results for back plane radiation patterns and would be useful for exploring the effects of a finite ground plane. It is not clear why the HFSS model produced such poor radiation calculations so further investigation is required. The results presented may be more sensitive to the size and shape of the radiation boundary than observed to date so that more parameter studies are required. Increasing the radiation boundary and refining the mesh further requires significantly more computation time so that even if better accuracy could be obtained, the simulations would be highly inefficient compared to the speed of EMP. For radiation pattern data, EMP provides a sufficiently accurate depiction of the front plane pattern with an idealized back plane pattern. HFSS may be useful for finite size planar antennas and antenna arrays but care must be taken to obtain a sufficiently refined model and a full convergence study would be required. With HFSS such an effort may not be justified for obtaining better accuracy compared to a 2.5-D model such as EMP which is reasonable accurate, fast, and has been successfully used for the design of aperture-coupled patch antenna arrays.

7. References

- 1 EMAG Technologies Inc., EMPiCASSO, <http://www.emagware.com/empicasso.html>, 2006.
- 2 Ansoft Corporation, High Frequency Structure Simulator (HFSS), <http://www.ansoft.com/products/hf/hfss/>, 2006.
- 3 Rogers Corp., Advance Circuit Materials Division Data Sheet, www.rogerscorporation.com, 2006.
- 4 Weiss, S.; Leshchyshyn, A. *Anechoic Chamber Upgrade*; ARAED-TR-95009; Army Armament RDEC, May 1995.

Distribution List

ADMNSTR
DEFNS TECHL INFO CTR
ATTN DTIC-OCP (ELECTRONIC COPY)
8725 JOHN J KINGMAN RD STE 0944
FT BELVOIR VA 22060-6218

DARPA
ATTN IXO S WELBY
3701 N FAIRFAX DR
ARLINGTON VA 22203-1714

OFC OF THE SECY OF DEFNS
ATTN ODDRE (R&AT)
THE PENTAGON
WASHINGTON DC 20301-3080

US ARMY TRADOC
BATTLE LAB INTEGRATION & TECHL
DIRCTRT
ATTN ATCD-B
10 WHISTLER LANE
FT MONROE VA 23651-5850

SMC/GPA
2420 VELA WAY STE 1866
EL SEGUNDO CA 90245-4659

COMMANDING GENERAL
US ARMY AVN & MIS CMND
ATTN AMSAM-RD W C MCCORKLE
REDSTONE ARSENAL AL 35898-5000

US ARMY INFO SYS ENGRG CMND
ATTN AMSEL-IE-TD F JENIA
FT HUACHUCA AZ 85613-5300

US ARMY SIMULATION TRAIN &
INSTRMNTN CMND
ATTN AMSTI-CG M MACEDONIA
12350 RESEARCH PARKWAY
ORLANDO FL 32826-3726

US GOVERNMENT PRINT OFF
DEPOSITORY RECEIVING SECTION
ATTN MAIL STOP IDAD J TATE
732 NORTH CAPITOL ST., NW
WASHINGTON DC 20402

US ARMY RSRCH LAB
ATTN AMSRD-ARL-CI-OK-TP
TECHL LIB T LANDFRIED (2 COPIES)
BLDG 4600
ABERDEEN PROVING GROUND MD
21005-5066

DIRECTOR
US ARMY RSRCH LAB
ATTN AMSRD-ARL-RO-EV W D BACH
PO BOX 12211
RESEARCH TRIANGLE PARK NC 27709

US ARMY RSRCH LAB
ATTN AMSRD-ARL-CI-OK-T
TECHL PUB (2 COPIES)
ATTN AMSRD-ARL-CI-OK-TL
TECHL LIB (2 COPIES)
ATTN AMSRD-ARL-D J M MILLER
ATTN AMSRD-ARL-SE-RE
T ANTHONY
ATTN AMSRD-ARL-SE-RM
C PATTERSON
ATTN AMSRD-ARL-SE-RM S KELLER
ATTN AMSRD-ARL-SE-RM
W O COBURN
ADELPHI MD 20783-11197

INTENTIONALLY LEFT BLANK.